Supporting Information

Fischbach *et al.* 10.1073/pnas.0808932106

SI Materials and Methods

Characterization of 2D and 3D Cell Cultures. Cell adhesion and proliferation were measured via fluorometric Hoechst 33258 DNA assay. For antibody inhibition studies, cells were preincubated with 5 μg/mL anti-$\alpha5\beta1$ (clone JBS5) and anti-$\alpha v\beta3$ (clone LM609) (both from Millipore). Cell viability was assayed by using a Vi-Cell analyzer (Beckmann Coulter), and histological characterization was carried out by H&E and Hypoxyprobe staining (Chemicon). For flow cytometry, anti-human $\alpha5$ and $\beta1$ antibody (BD Biosciences) and Alexa Fluor 488-conjugated IgG (Molecular Probes) were used. FRET analysis of bond formation between cells and 3D RGD-alginate substrates was performed as described in ref. 1.

Analysis of Angiogenic Factor Expression. Bascular endothelial growth factor (VEGF)(165), basic fibroblast growth factor (bFGF), and IL-8 ELISAs (R&D) were performed according to the manufacturer's instructions; values were normalized to cell numbers as determined by Hoechst 33258 DNA assay. To analyze factor secretion in response to different ECM proteins, OSCC-3 were seeded under serum-free conditions in tissue culture plastic (TCPS) dishes and culture dishes coated with fibronectin (20 μg/mL). To analyze angiogenic factors deposited within the matrices, alginate substrates were dissolved in 50 nM EDTA/PBS, and these solutions were subjected to analysis. Control experiments using alginase treatment yielded similar results and verified no interference of dissolved alginate with ELISA analysis. Angiogenic proteins from in vivo tumors were extracted by tissue homogenization with TPER lysis buffer (Pierce), measured by ELISA, and standardized for total protein content as determined by Bio-Rad protein assay. Systemic concentrations of angiogenic factors were determined by ELISA of serum samples collected before tumor harvest from SCID mice.

Analysis of Growth Factor Diffusion. The mathematical diffusion model describes the spatial distribution profiles of VEGF and IL-8 in the tissue surrounding OSCC-3 tumors as a result of diffusion, elimination, and secretion. Because both factors are heparin-binding (2, 3) and it remains unclear whether the binding affinity varies with the two factors, it was assumed that the effect of VEGF and IL-8 binding to the ECM was similar with the two factors. The governing equations of the VEGF and IL-8 concentration, c_V and c_I, in the tumor were:

$$\frac{\partial c_V}{\partial t} = D_V \nabla^2 c_V - k_{eV} c_V + R_V \qquad [s1]$$

$$\frac{\partial c_I}{\partial t} = D_I \nabla^2 c_I - k_{eI} c_I + R_I \qquad [s2]$$

The governing equations of c_V and c_I in the surrounding tissue were:

$$\frac{\partial c_V}{\partial t} = D_V \nabla^2 c_V - k_{eV} c_V \qquad [s3]$$

$$\frac{\partial c_I}{\partial t} = D_I \nabla^2 c_I - k_{eI} c_I \qquad [s4]$$

The diffusion coefficient of VEGF ($D_V = 7.0 \times 10^{-7}$ cm^2/s) and IL-8 ($D_I = 2.5 \times 10^{-6}$ cm^2/s) were derived from the literature (4, 5). The generation terms R_V and R_I were determined in vitro by using an engineered OSCC-3 tumor model and confirmed in vivo after implantation of the model system in vivo (C.F., H.J.K., S.X.H., W.Y., M.B.E., D.J.M., unpublished work). The elimination rates of VEGF (k_{eV}) and IL-8 (k_{eI}) were based on the literature [$t_{1/2,\,VEGF}$ = 13.8 min, $t_{1/2,\,IL\text{-}8}$ = 10 min (6, 7)]. The steady-state system was solved in COMSOL Multiphysics by using the 3D coefficient form PDE solver with direct UMFPACK method. Fluorescence labeling of VEGF and IL-8 was performed with a Alexa Fluor 555 microscale protein labeling kit (Molecular Probes). The degrees of labeling and yield were determined according to equations provided in the instructions, and the determined values were used for normalization of fluorescence intensity. Diffusion studies were conducted by injection of protein solutions into phenol red-free Matrigel and fluorescence imaging at 12.5-fold magnification. Matrigel instead of alginate was used in this work to mimic the ECM in tumors in vivo more accurately. ImageJ was used to perform densitometric image analysis.

Analysis of Tumor Growth in Vivo. OSCC-3 were mixed with RGD-alginate solutions (2% wt/wt in DMEM) to yield a density of 1.5 million cells per implant. For inhibition studies, these suspensions were combined with neutralizing VEGF antibody (50 μg per 200 μL of implant; R&D) and/or neutralizing IL-8 antibody (100 μg per 200 μL of implant; R&D) before cross-linking. According to the neutralization dose$_{50}$ (ND$_{50}$) indicated by the manufacturer, VEGF blocking antibody is ≈5-fold more potent than the IL-8 blocking antibody, and it was, therefore, used at lower concentrations. Mice from one experimental group were treated with i.p. injections of VEGF and IL-8 antibodies instead of localized delivery from alginate gels. OSCC-3/RGD-alginate suspensions were cross-linked with $CaSO_4$ and immediately injected into s.c. pockets in the back of male, 6- to 8-week old, immunocompromised CB17 SCID (for human OSCC-3; Taconic). Implants were retrieved and measured after 3 weeks; 4–6 tumors were analyzed per experimental group.

Implantation of Scaffolds into EGFP$^+$ Bone Marrow-Transplanted Mice. For bone marrow transplantation, C57BL/6J were lethally irradiated (10 Gy) and transplanted with 4 million bone marrow cells harvested from EGFP-transgenic mice [C57BL/6-TgN(ActbEGFP)1Osb/J (8); D.J.M.'s breeding colony at Harvard University]. Four control scaffolds and six IL-8-releasing scaffolds were implanted 6 weeks after the bone marrow transplant by making one small incision and creating two spatially separated pockets to insert two constructs of the same experimental group per mouse.

Histological Analysis of Blood Vessels. To identify blood vessels, paraffin sections were subjected to proteinase K (Dako) antigen retrieval and were subsequently immunostained with antibodies raised against mouse CD31 (PharMingen) by using the TSA biotin system (PerkinElmer) and anti-rat secondary antibody (Vector Laboratories). Blood vessel density was analyzed by capturing digital images of tissue sections along the muscle–scaffold interface and quantifying the number of vessels located between the scaffold and the muscle; values were normalized to the length of the muscle–scaffold interface as determined by image analysis using ImageJ. To quantify CD31/GFP$^+$ cells, cryosections were double-stained by using anti-mouse CD31 IgG (clone MEC13.3; BD Biosciences) in conjunction with Alexa

Fluor 647 anti-rat IgG (Invitrogen) and Alexa Fluor 555-conjugated anti-GFP IgG (Invitrogen) to circumvent difficulties associated with bleaching of GFP (colocalization of staining was confirmed; Fig. S9); DAPI (Invitrogen) was used for counterstaining. Images of optical sections of immunostained cryosections were taken at the muscle–scaffold interface at a 200× magnification with an ApoTome camera (Zeiss) mounted to an inverted fluorescent microscope (AxioObserver Z1; Zeiss), and AxioVision software (Zeiss) was used for image analysis of costaining.

Statistical Analysis. Statistical significance of data were assessed by using one-way ANOVA for the respective experiment followed by a post hoc comparison by using the Tukey test. Four independent experiments were performed for each condition tested in vitro (sample number $n = 4$). Statistical significance between control and experimental conditions of in vivo samples was tested with $n = 4$ and $n = 8$ samples for antibody delivery studies and IL-8 delivery in GFP bone marrow transplant experiments, respectively. In all figures, values are reported as the mean, and error bars indicate standard deviations (*, $P < 0.05$; **, $P < 0.01$ between noted conditions).

1. Kong HJ, Boontheekul T, Mooney DJ (2006) Quantifying the relation between adhesion ligand–receptor bond formation and cell phenotype. *Proc Natl Acad Sci USA* 103:18534–18539.
2. Goerges AL, Nugent MA (2003) Regulation of vascular endothelial growth factor binding and activity by extracellular pH. *J Biol Chem* 278:19518–19525.
3. Kuschert GS, *et al.* (1998) Identification of a glycosaminoglycan binding surface on human interleukin-8. *Biochemistry* 37:11193–11201.
4. Helm CL, Fleury ME, Zisch AH, Boschetti F, Swartz MA (2005) Synergy between interstitial flow and VEGF directs capillary morphogenesis in vitro through a gradient amplification mechanism. *Proc Natl Acad Sci USA* 102:15779–15784.
5. Moghe PV, Nelson RD, Tranquillo RT (1995) Cytokine-stimulated chemotaxis of human neutrophils in a 3D conjoined fibrin gel assay. *J Immunol Methods* 180:193–211.
6. Hsei V, Deguzman GG, Nixon A, Gaudreault J (2002) Complexation of VEGF with bevaczumab decreases VEGF clearance in rats. *Pharm Res* 19:1753–1756.
7. Gaertner HF, Offord RE (1996) Site-specific attachment of functionalized poly(ethylene glycol) to the amino terminus of proteins. *Bioconjug Chem* 7:38–44.
8. Okabe M, Ikawa M, Kominami K, Nakanishi T, Nishimune Y (1997) ''Green mice'' as a source of ubiquitous green cells. *FEBS Lett* 407:313–319.

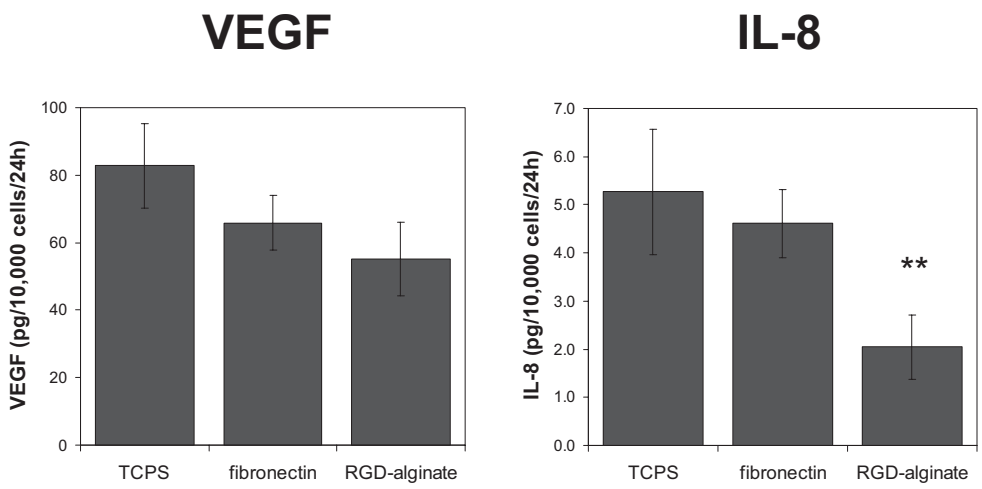

Fig. S1. Tumor cells cultured on 2D RGD-alginate substrates secreted VEGF at concentrations comparable with culture on TCPS and TCPS coated with fibronectin. IL-8 secretion was slightly down-regulated on 2D RGD-alginate substrates relative to conventional 2D cultures (**, $P < 0.01$), but IL-8 secretion rates were very low on all 2D matrices.

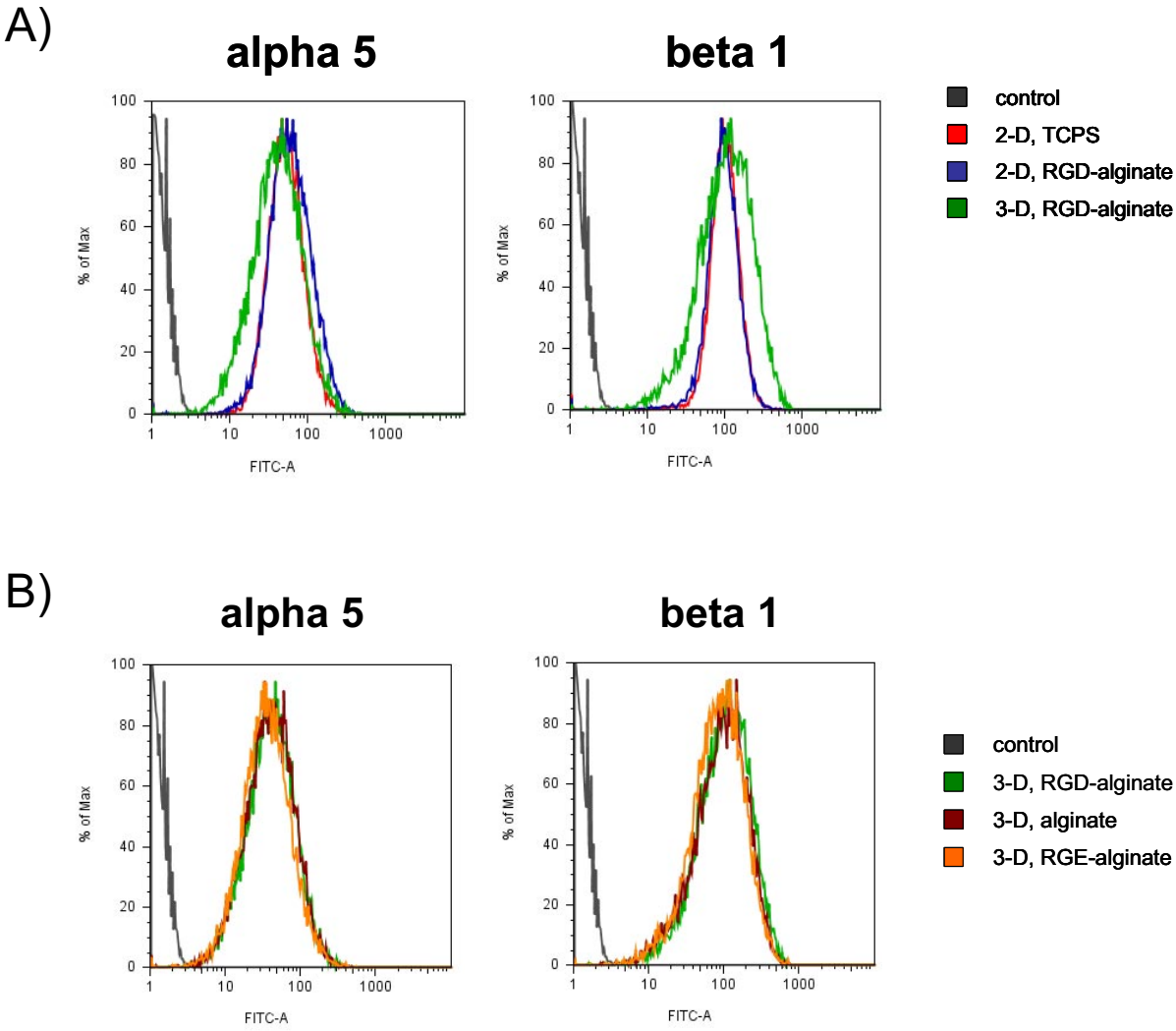

Fig. S2. Integrin expression of tumor cells cultured in 2D and 3D alginate systems. (*A*) FACS analysis of fibronectin receptor ($\alpha5\beta1$ integrin) expression revealed that 2D culture on RGD-alginate (2D, RGD-alginate) did not alter expression of $\alpha5$ and $\beta1$ subunits relative to conventional monolayer culture on TCPS (2D, TCPS). Three-dimensional culture within RGD-alginate (3D, RGD-alginate) slightly decreased $\alpha5$ and enhanced the variability of $\alpha5$ and $\beta1$ expression. (*B*) Expression of $\alpha5$ was not altered by 3D culture within artificial ECMs that mediated (3D, RGD-alginate) or prevented (3D, alginate; 3D, RGE-alginate) 3D integrin engagement. Two-dimensional precultured tumor cells without antibody served as controls (control) and confirmed specificity of staining.

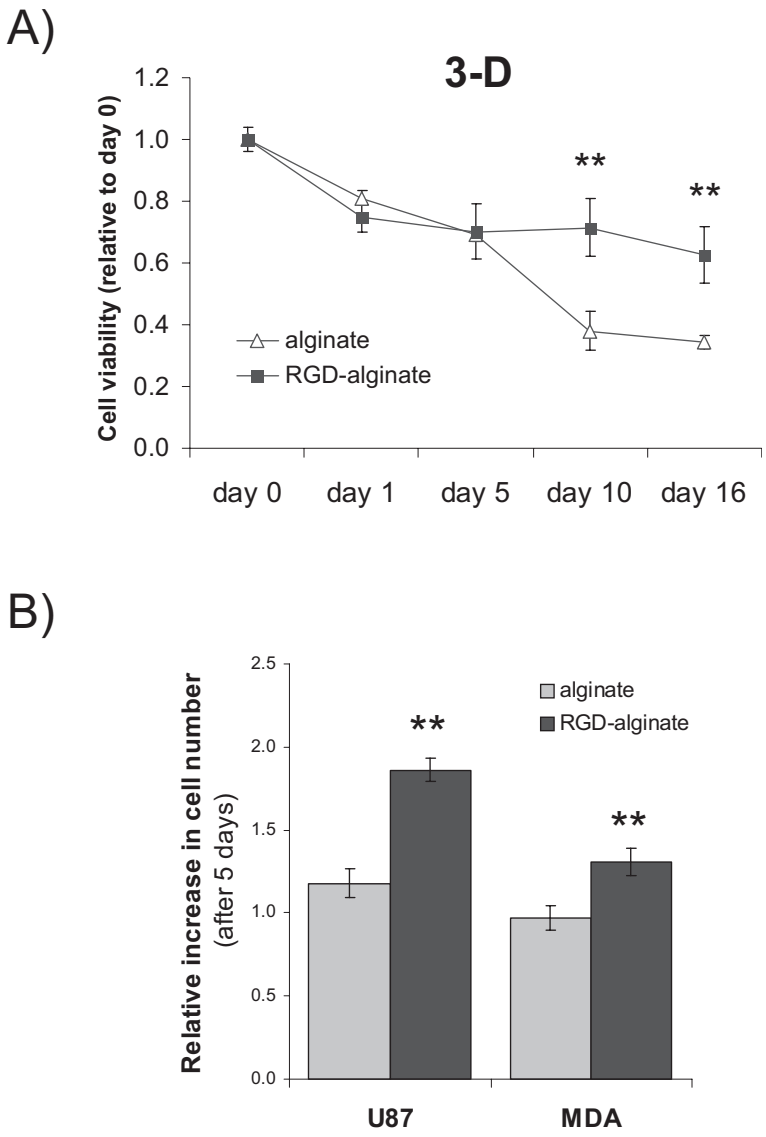

Fig. S3. Effects of 3D integrin engagement on cell viability and proliferation. (*A*) Integrin engagement mediated enhanced cell viability at later time points of 3D culture (**, $P < 0.01$). (*B*) Three-dimensional integrin engagement promoted cell proliferation of U87 brain cancer cells and MDA-MB231 breast cancer cells within RGD-modified alginate (RGD-alginate) relative to culture within unmodified alginate (alginate) (**, $P < 0.01$).

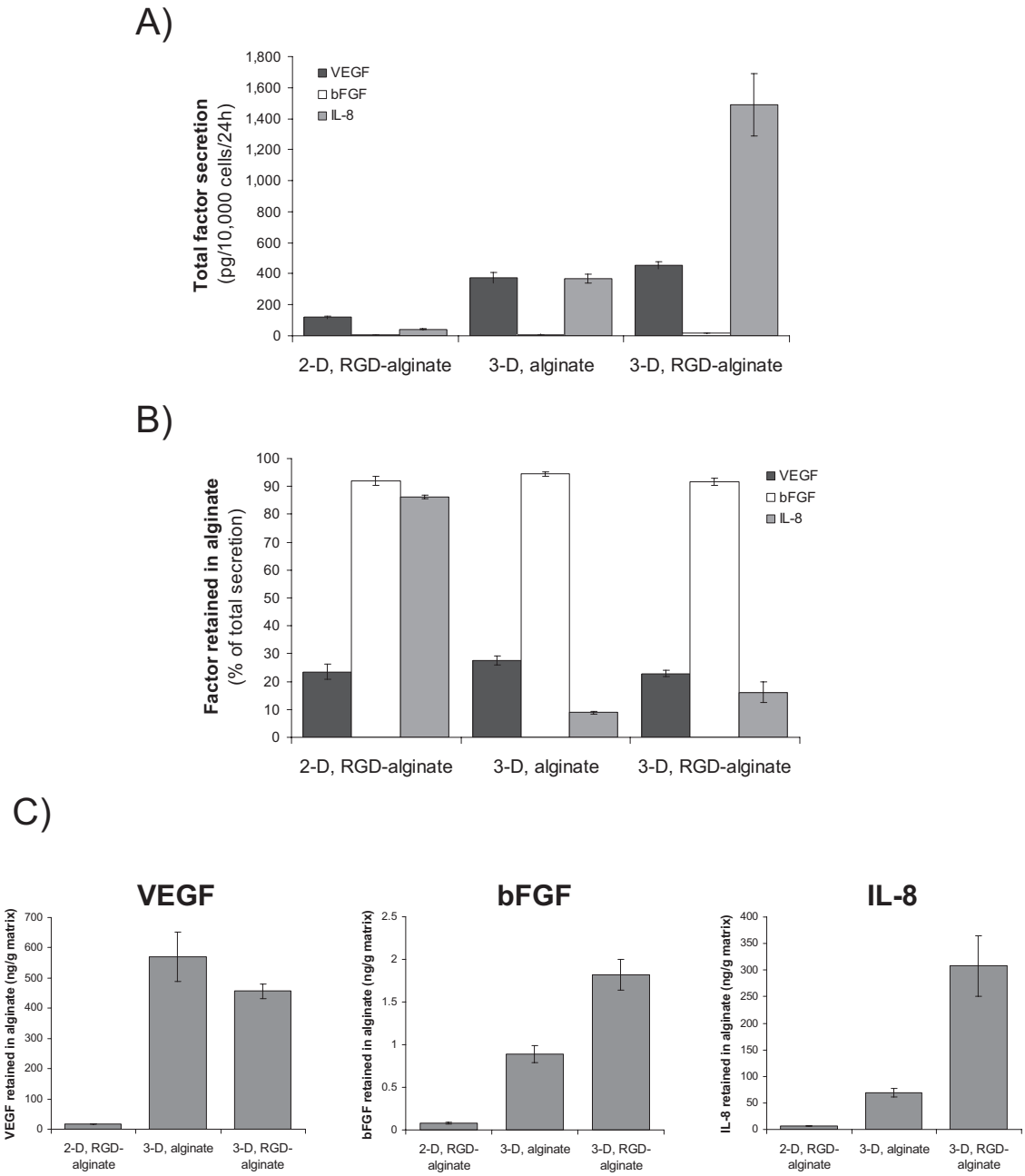

Fig. S4. Angiogenic capability of tumor cells cultured in 2D and 3D alginate systems. (*A*) Analysis of total factor secretion (i.e., sum of factor release into the culture medium and factor deposition within the used matrices) confirmed that IL-8 secretion was more remarkably regulated by 3D culture conditions and 3D integrin engagement than VEGF and that bFGF was secreted at negligibly low levels in all conditions. (*B*) Factor deposition within 2D and 3D alginate matrices. VEGF and bFGF sequestration within the different substrates was similar for all conditions, but bFGF was retained at a higher concentration than VEGF. IL-8 deposition was enhanced under 2D conditions (2D, RGD-alginate) compared with 3D culture conditions (3D alginate; 3D, RGD-alginate), an observation that may be attributed to the low secretion values under this condition. (*C*) Absolute amounts of angiogenic factors deposited in 2D and 3D artificial ECMs. When normalized to the absolute mass of the used materials, 2D RGD-alginate substrates (2D, RGD-alginate) contained remarkably smaller amounts of VEGF, bFGF, and IL-8 relative to 3D cultures (3D, alginate and 3D, RGD-alginate), suggesting that the detected differences in angiogenic factor concentration and retention are not caused by saturation of the factors in 2D vs. 3D gel matrices but are likely related to changes in angiogenic factor secretion.

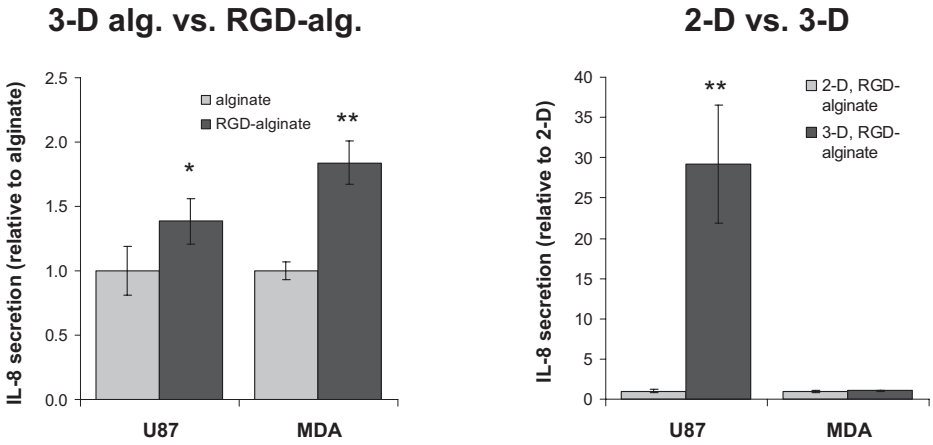

Fig. S5. U87 glioblastoma cells up-regulated IL-8 secretion in response to both 3D integrin engagement (3D, alginate vs. 3D, RGD-alginate) and 3D culture conditions (2D, RGD-alginate vs. 3D, RGD-alginate), whereas IL-8 secretion by MDA-MB231 breast cancer cells was only enhanced after 3D integrin engagement, but not because of 3D culture.

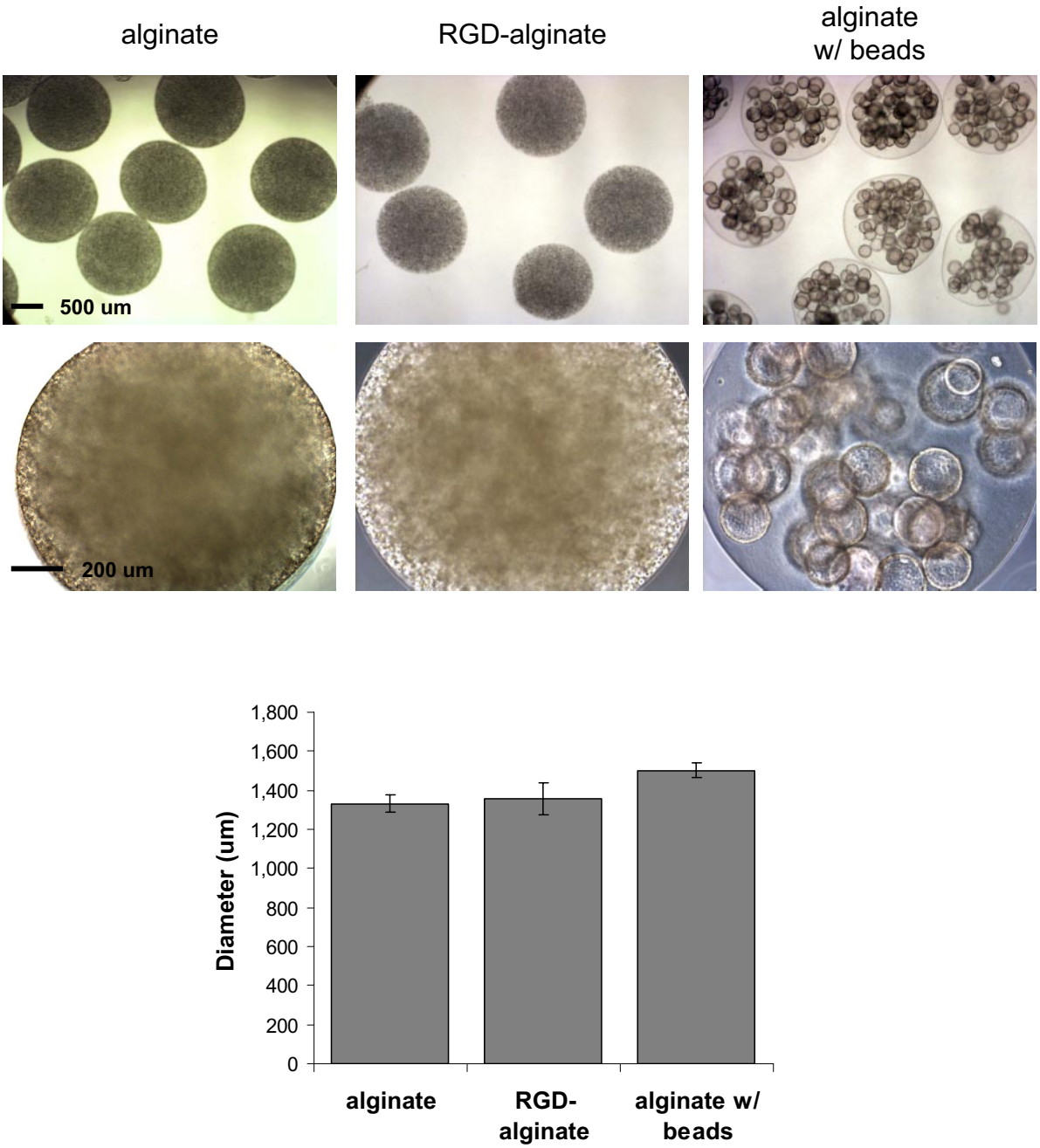

Fig. S6. Morphology and size of 3D cultures fabricated from alginate, RGD-alginate, and alginate encapsulated with cell-coated microcarrier beads (alginate w/beads) as visualized by light microscopy and analyzed by image analysis, respectively. Cells exhibited no adhesions in alginate cultures, 3D adhesions in RGD-alginate cultures, and 2D adhesions in alginate-bead cultures.

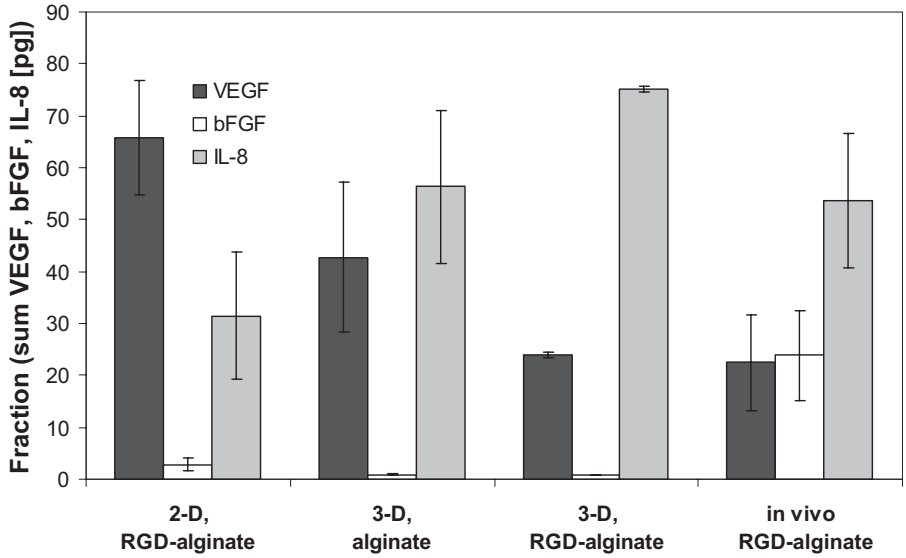

Fig. S7. VEGF, bFGF, and IL-8 secretion presented as a fraction of the total secretion of angiogenic factors (for in vitro studies: sum of factor released into the culture and deposited within the matrix; expressed in picograms per 10,000 cells). The effects of 3D microenvironmental conditions and 3D integrin engagement were determined by comparing 2D cultures on RGD alginate, 3D culture within alginate, and RGD-alginate, and tumors formed in vivo. Error bars are small where not visible.

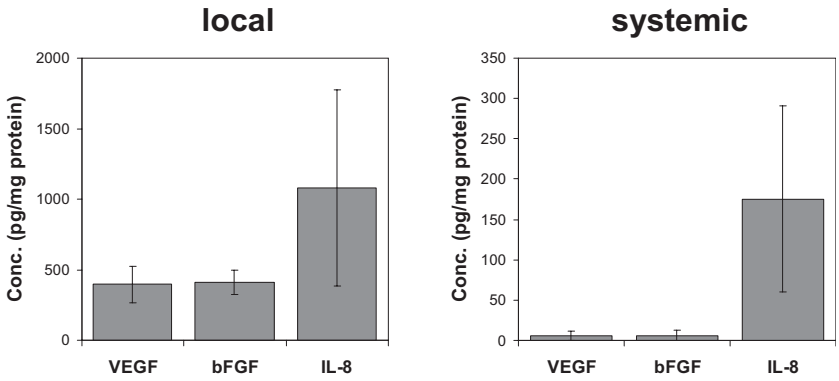

Fig. S8. Both local and systemic IL-8 concentrations were enhanced in vivo, relative to VEGF and bFGF, as determined by ELISA of tumor lysates and serum samples of tumor-bearing mice, respectively. Although a trend was found, these differences were not statistically significant.

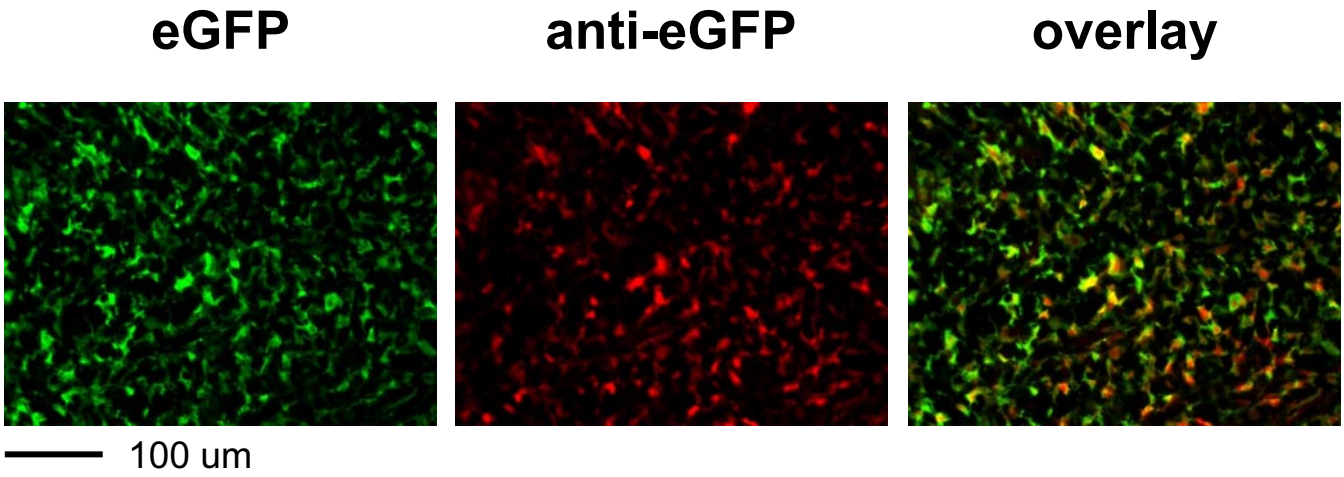

Fig. S9. Immunostaining of EGFP-labeled cells with an Alexa Fluor 555-conjugated anti-GFP antibody prevented difficulties associated with EGFP photobleaching, and overlay of images taken from freshly cut cryosections (EGFP) and cryosections exposed to antibody staining (anti-EGFP) confirmed specificity of staining.